Chinese Journal of
POLYMER SCIENCE

RESEARCH ARTICLE

https://doi.org/10.1007/s10118-026-3790-7
Chinese J. Polym. Sci.

Constructing Superhydrophobic High-internal-phase Emulsion Fluoro-coatings from Hydrophilic Polyoxometalates for Durable Photochromic Functionality

Pei-Ze Yang[a,b], Xiao-Shuang Li[a,b], Bo-Yu Lei[a,b], Yi-Lin Tang[a,b], Bing Geng[a,b*], Guang-Hui Cui[c*], and Mei Yan[a,b*]

[a] *School of Chemistry and Chemical Engineering, University of Jinan, Jinan 250022, China*
[b] *Shandong Provincial Key Laboratory of Extreme Environment-tolerant Specialty Chemicals, University of Jinan, Jinan 250022, China*
[c] *Drilling Fluid Research Center of Mud Service Branch, Bohai Drilling Engineer Company, China National Petroleum Corporation (CNPC), Tianjin 300280, China*

Electronic Supplementary Information

Abstract Integrating photoresponsive components into superhydrophobic surfaces remains a challenge because functional species often disrupt the hierarchical micro/nanostructures required for superhydrophobicity. In particular, intrinsically hydrophilic polyoxometalates (POMs) are difficult to incorporate into low-surface-energy systems without compromising their structural integrity and wetting performance. Herein, a fluoropolymer porous coating of phosphomolybdic acid (FPPC@PMA) was fabricated *via* a high-internal-phase emulsion (HIPE) templating strategy, enabling the simultaneous immobilization of hydrophilic POMs and construction of a hierarchical porous fluoropolymer framework. The resulting FPPC@PMA coating exhibited excellent superhydrophobicity with a water contact angle of 152° and remarkable mechanical durability in sandpaper abrasion and tape-peeling tests. Owing to the redox activity of PMA, the composite also displays a sensitive and reversible photochromic response upon ultraviolet irradiation, suggesting its potential applications in ultraviolet (UV) monitoring and information encryption. Molecular dynamics simulations further elucidated the interfacial interactions between the polymer matrix and phosphomolybdic acid clusters, providing theoretical insights into the structural stability of the composite system. This work offers an effective strategy for integrating hydrophilic photoresponsive species into superhydrophobic architectures while maintaining their structural integrity and functionality.

Keywords HIPE-templated coatings; Multifunctional fluoropolymers; Superhydrophobic interfaces; Photochromism

Citation: Yang, P. Z.; Li, X. S.; Lei, B. Y.; Tang, Y. L.; Geng, B.; Cui, G. H.; Yan, M. Constructing superhydrophobic high-internal-phase emulsion fluoro-coatings from hydrophilic polyoxometalates for durable photochromic functionality. *Chinese J. Polym. Sci.* https://doi.org/10.1007/s10118-026-3790-7

INTRODUCTION

The development of bio-inspired intelligent interfacial materials with integrated self-sensing and dynamic feedback capabilities has emerged as a pivotal research direction for realizing functional adaptability in complex environments.[1] Conventional superhydrophobic surfaces exhibit excellent self-cleaning and antifouling properties, they are primarily limited to passive protection and lack the ability to respond to external stimuli (*e.g.*, light, electricity, and heat) in real time or enable information exchange or encryption.[2] Therefore, integrating light-responsive functionalities, such as UV mask-assisted patterning, into superhydrophobic systems has become an important strategy for constructing next-generation intelligent interfaces.[3] However, integrating photoresponsive species into superhydrophobic systems remains challenging because the incorporation of functional components often compromises the hierarchical micro/nanostructures required for superhydrophobicity, resulting in reduced structural stability and functional performance.

Polyoxometalates (POMs) exhibit unique advantages as photochromic materials, owing to their reversible photoinduced redox properties.[4] However, POMs are highly soluble in polar media and often exhibit poor dispersion stability. When directly introduced into polymer matrices, they tend to aggregate, leach out, or exhibit insufficient interfacial compatibility, thereby reducing structural stability and photoresponse efficiency.[5] Moreover, the incorporation of functional components into superhydrophobic systems may disrupt the original hierarchical micro/nanostructures, resulting in reduced surface roughness and mechanical durability.[6] Consequently, achieving the synergistic integration of stable POM immobilization and robust superhydrophobic structures within a single-material system remains challenging. The fundamental scientific challenge lies in resolving the inherent trade-off and thermodynamic incompatibility between intrinsically hydrophilic functional clusters and low surface energy

* Corresponding authors, E-mail: chm_gengb@ujn.edu.cn (B.G.)
E-mail: cuiguanghui@cnpc.com.cn (G.H.C.)
E-mail: chm_yanm@ujn.edu.cn (M.Y.)
Received May 7, 2026; Accepted June 17, 2026; Published online September 29, 2026

matrix networks. Conventional composite strategies such as simple physical blending or spray coating often rely on weak interfacial adhesion or uncontrolled random stacking. These conventional methods frequently fail to maintain biomimetic hierarchical roughness while ensuring stable functional loading, leading to severe component leaching, pore clogging, and functional failure under external mechanical stress.[7]

To address these challenges, the high internal phase emulsion (HIPE) templating strategy provides an effective approach for constructing three-dimensional interconnected porous structures and regulating the interfacial distribution of functional components.[8] Distinct from traditional surface-coating methods that form superficial, vulnerable layers, the highly porous polymer network derived from HIPE creates a continuous, monolithic, three-dimensional skeleton. This interconnected network not only offers abundant interfacial sites for chemically anchoring and sequestering functional species within the matrix walls, but also helps maintain an interconnected micro/nano hierarchical roughness that is favorable for stable, superhydrophobic surfaces.[9] In conventional coatings, functional roughness is typically confined to the outermost surface and can be readily removed during mechanical wear. In contrast, the self-similar porous skeleton generated by the HIPE process preserves the hierarchical roughness throughout the bulk material, allowing the newly exposed surfaces to retain superhydrophobic characteristics even after abrasion. Fluoropolymers are considered ideal materials for constructing superhydrophobic interfaces because of their intrinsically low surface energies.[10,11] Based on this concept, incorporating POMs into HIPE-derived fluorinated porous polymer networks could enable their stable immobilization *via* interfacial interactions. The hierarchical porous structure was preserved, imparting reversible photochromic properties while maintaining excellent superhydrophobic performance and achieving the synergistic integration of wettability control and photoresponsive functionality.

In this study, a multifunctional fluoropolymer-supported phosphomolybdic acid coating (FPPC@PMA) was fabricated using the HIPE templating strategy. In this system, an oil phase composed of polyurethane diacrylate (PUDA) and the fluorinated monomer HFBA encapsulates an aqueous phosphomolybdic acid solution to form a stable water-in-oil (W/O) emulsion. After polymerization, a biomimetic hierarchical porous structure was obtained, in which PMA clusters were uniformly immobilized within the fluorinated polymer matrix. The resulting coating exhibited excellent superhydrophobicity with a static water contact angle of 152° and remarkable mechanical durability in sandpaper abrasion and tape-peeling tests. Furthermore, redox-active PMA endowed the coating with a sensitive and reversible photochromic response under UV irradiation, enabling its application in UV detection and information encryption. To further understand the origin of the structural stability, molecular dynamics (MD) simulations were conducted to elucidate the interfacial interactions between the polymer chains and PMA clusters, providing theoretical insights into the stability and uniformity of the composite structure. This study offers a general strategy for developing intelligent, durable, and multifunctional surfaces that are suitable for harsh environments.

EXPERIMENTAL

Materials

2,2,3,4,4,4-Hexafluorobutyl acrylate (HFBA 98%) was obtained from Harbin Saiojia FluoroSilicon Chemical Co., LTD., (Harbin, China). 2-Ethylhexyl acrylate (2-EHA) was obtained from Shanghai Aladdin Bio-Chem Technology Co., Ltd., (Shanghai, China). Hypermer B246, a copolymer consisting of poly(hydroxy stearic acid) and poly(ethylene glycol), was supplied by Croda, USA. Poly(urethane diacrylate) PUDA (EBECRYL® 284) is an aliphatic poly(urethane diacrylate) oligomer diluted with 1,6-hexanediol diacrylate monomer, supplied by Cytec Company, Belgium. Phosphomolybdic acid (PMA) and AIBN were obtained from Aladdin. All chemicals were used without further purification.

Preparation of FPPC@PMA

First, accurately weigh 0.48 g of Hypermer B246, 1.1 g of HFBA, 3.6 g of EHA and 3.2 g of PUDA to form the oil phase. Then, add 0.1 g of AIBN as a thermal initiator. After ultrasonic treatment of the mixed oil phase for 10 min to ensure thorough mixing, the mixture was transferred to a 100 mL three-necked flask. Under uniform stirring at 500 r/min, 23 mL of 0.08 mol/L phosphomolybdic acid aqueous solution was gradually added to the oil phase, eventually forming a stable W/O type high internal phase emulsion. After polymerization at 60 °C for 12 h, the obtained monolith was thoroughly washed with ethanol for several times to remove the residual surfactant and unreacted species, followed by vacuum drying at 60 °C for 12 h.

Characterizations

Fourier infrared spectroscopy (FTIR) (Nicolet iS10, USA) was measured within a 4000–500 cm^{-1} scanning range. A scanning electron microscope (SEM) (Gemini300, Germany) was used to analyze the microscopic morphology of the surface and cross-section of the FPPC@PMA. The samples for the cross-sectional scanning electron microscope characterization were prepared by careful snapping after immersion in liquid nitrogen for 30 s. The content and distribution of elements on the surface of FPPC@PMA were characterized by energy-dispersive X-ray spectroscopy (EDS) with a secondary electron mode and an accelerating voltage of 20 kV (X-MAX-50, UK). The morphology and structure of FPPC@PMA were observed by transmission electron microscopy (TEM, FEI-Tecnai 12). The hydrophobicity of FPPC@PMA was measured at room temperature using a fully automated optical video contact-angle measuring device OCA40 (Data Physics, Germany). X-ray photoelectron spectroscopy (XPS) was performed using a Thermo EscaLab 250Xi (USA) with an Al Kα source (15 kV and 25 W) and a pass energy of 100 eV to analyze the surface elements of FPPC@PMA. The absorption spectra were recorded using a UV-Vis-NIR spectrophotometer (Shimadzu, UV-3600 Plus) from 200 nm to 400 nm with an integrating sphere. Absorbance (A) can be calculated as $A = 1 - R - T$, where R and T are the reflection and transmission, respectively.

Molecular Dynamics Simulation

The interactions between phosphomolybdic acid (PMA) and the polymer at their interfaces were examined using molecular dynamics (MD) simulations. The Forcite module in Materials Studio was used to set up the polymer-PMA systems through the Amorphous Cell module, the force field was the Universal

https://doi.org/10.1007/s10118-026-3790-7

Force field, the system used an NVT ensemble, and the charge distribution method was QEQ assigned. The temperature was set at 25 °C, and the total simulation duration was set to 200 ps, with a time step of 1 fs. The interactions between PMA and the polymer were analyzed over a period of 1–200 ps. In total, 200 interaction instances were computed.

RESULTS AND DISCUSSION

Characterization of FPPC@PMA

A high internal phase emulsion (HIPE) was constructed using a fluoropolymer-containing oil phase and an aqueous phase containing phosphomolybdic acid (FPPC@PMA) (Fig. 1). During emulsification, PMA was enriched at the oil-water interface and subsequently immobilized within the fluoropolymer matrix upon polymerization, forming a porous FPPC@PMA coating. The hierarchical micro/nanostructure derived from the HIPE template, together with low-surface-energy fluorinated segments, imparts superhydrophobicity by maintaining the water droplets in a Cassie state. Under UV irradiation, redox-active PMA undergoes a photoinduced electronic transition (Mo^{6+}/Mo^{5+}conversion), leading to an optical response that enables UV detection. The bottom panel shows the chemical structures of the polyurethane diacrylate, hexafluorobutyl acrylate, 2-ethylhexyl acrylate, and phosphomolybdic acid used in the composite system.

In this study, we successfully prepared fluoropolymer-supported polyoxometalate (POMs) superhydrophobic photochromic coating materials using a high internal phase emulsion (HIPE) templating method. Figs. 2(a) and 2(b) show scanning electron microscope (SEM) images of the samples, clearly demonstrating the biomimetic lotus leaf-like micro-nano hierarchical structure of the material. Fig. 2(a) shows that the material surface exhibits a three-dimensional interconnected porous network structure, with pore diameters mainly distributed in the range of 1–3 μm. This micron-level rough structure is the key framework for achieving superhydrophobic properties. To quantitatively evaluate the uniformity of the HIPE-derived porous structure, pore-size statistics were obtained from the SEM images. As shown in Fig. S2 (in the electronic supplementary information, ESI), the pores are distributed within a relatively narrow size range, indicating good structural homogeneity throughout the porous framework. Such a uniform porous architecture is beneficial for maintaining consistent surface roughness and contributes to the excellent superhydrophobic performance of the coating. The high-magnification SEM image (Fig. 2b) further reveals that nanoscale clusters were uniformly distributed on the pore walls of the porous skeleton. These nanostructures, together with the micron-level channels, form a micro-nano composite rough morphology similar to the lotus leaf surface, providing a structural basis for superhydrophobic perfor-

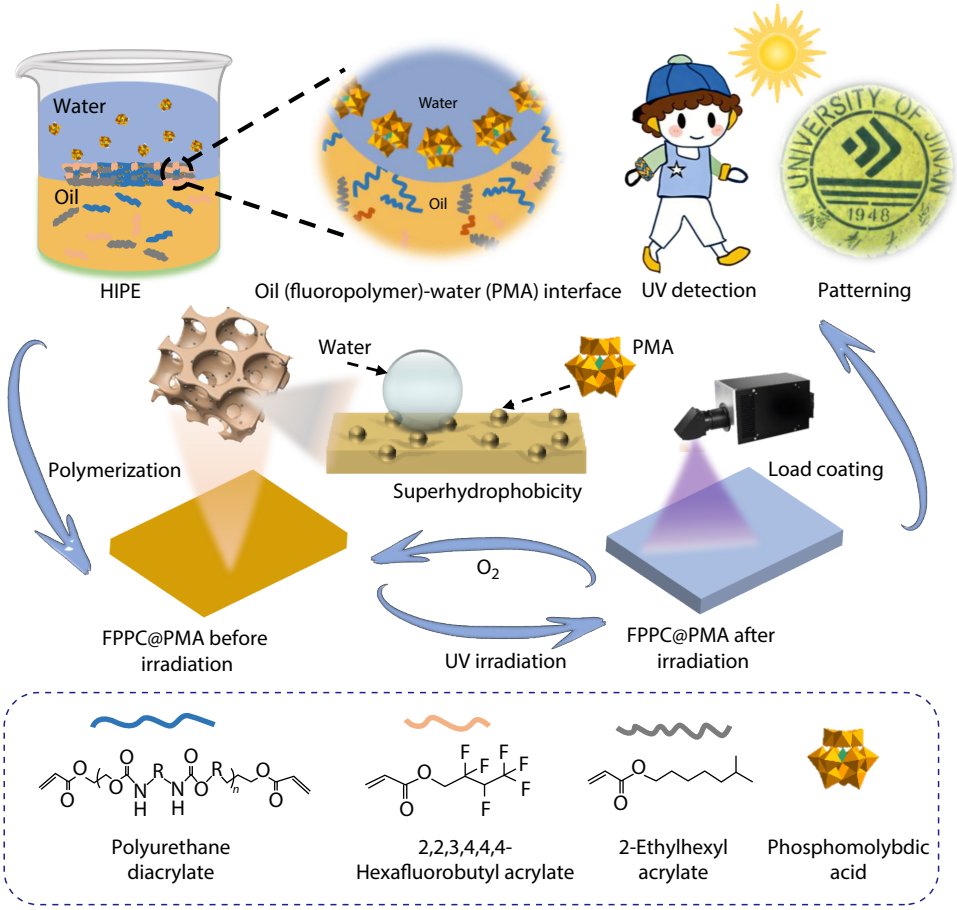

Fig. 1 Schematic illustration of the fabrication process and multifunctional mechanism of the FPPC@PMA coating.

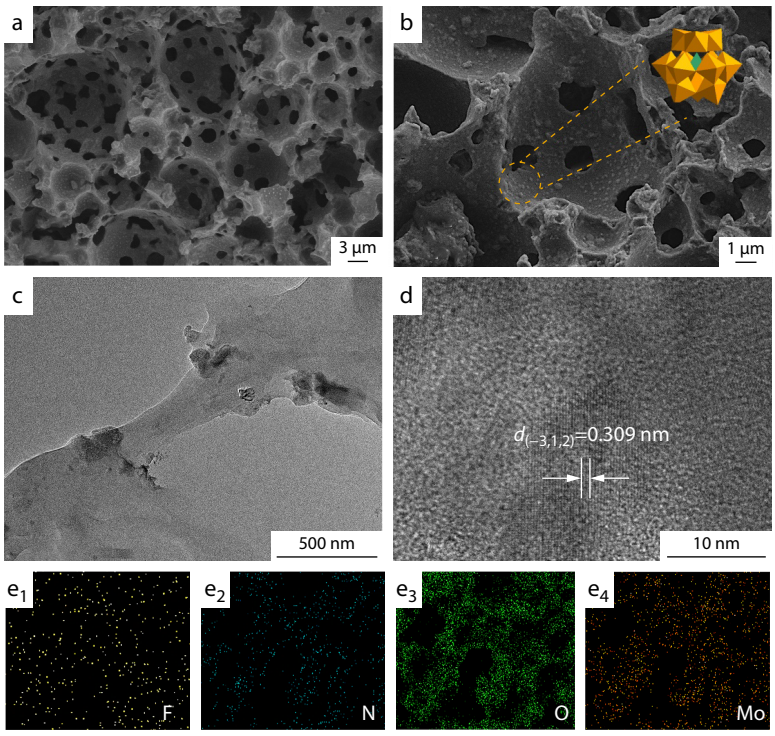

Fig. 2 Morphological and elemental characterization of the composite coating. (a, b) SEM images at different magnifications; (c) TEM image; (d) HRTEM image; (e_1–e_4) EDS elemental mapping images of F, N, O, and Mo.

mance.[1] To evaluate the influence of PMA incorporation on the hierarchical porous structure, a blank HIPE fluoropolymer sample (FPPC) without PMA was prepared as a control. As shown in Fig. S1 (in ESI), both FPPC and FPPC@PMA exhibit typical interconnected porous morphologies derived from the HIPE template, and no obvious pore collapse or structural disruption is observed after PMA incorporation. The pore size distribution analysis further revealed only minor variations in the average pore diameter, suggesting that the introduction of PMA does not significantly alter the HIPE-derived porous framework. This indicates that the HIPE polymerization process can effectively immobilize hydrophilic PMA within the fluoropolymer network while preserving the hierarchical micro/nano roughness essential for superhydrophobicity. Fig. 2(c) shows the typical two-dimensional lamellar morphology of the fluoropolymer matrix with distinct wrinkles between the layers. This structural characteristic facilitates an increase in the specific surface area and provides ample sites for the loading polyoxometalates (POMs). The high resolution transmission electron microscope (HRTEM) image (Fig. 2d) reveals clear lattice fringes with a spacing of d=0.309 nm, corresponding to the (−3,1,2) plane, confirming the successful loading and good crystallinity of the POMs on the fluoropolymer surface. Furthermore, the uniformly distributed nanocrystalline structure enhances the surface roughness of the material.

To confirm the elemental composition and spatial distribution, energy-dispersive X-ray spectroscopy (EDS) mapping was performed on the samples (Figs. 2e_1–2e_4). Analysis demonstrated that fluorine (F, derived from the fluoropolymer), nitrogen (N), oxygen (O, originating from polyoxometalates and polymer functional groups), and molybdenum (Mo, the central metal in polyoxometalates) were uniformly distributed throughout the sample area without any evident elemental aggregation. This homogeneity not only ensures the full exposure of low-surface-energy C—F bonds on the coating surface but also facilitates the effective utilization of photochromically active sites in POMs, thereby providing a chemical basis for the multifunctionality of the coating.

The elemental compositions of the coatings were first examined using XPS survey spectra (Fig. 3a). Both the FPPC and FPPC@PMA samples exhibited characteristic C 1s, O 1s, and F 1s signals, confirming the successful construction of the fluoropolymer framework. After loading the polyoxometalates, an additional Mo 3d signal appeared in FPPC@PMA, verifying the successful incorporation of the POM species into the porous fluoropolymer matrix.

The high-resolution Mo 3d spectrum (Fig. 3b) can be deconvoluted into multiple components corresponding to Mo^+ and partially reduced Mo^+ species. The coexistence of these valence states suggests electron transfer interactions between the fluoropolymer matrix and POM clusters, which are beneficial for the photochromic activity. Compared to pristine PMA, the broadened peaks in FPPC@PMA indicate strong interfacial coupling and stable POM immobilization. The N 1s spectra (Fig. 3c) reveal the presence of —NH—, protonated —NH_2^+, and C—N species.[12] After POM loading, the peak positions shifted slightly, suggesting hydrogen bonding or electrostatic interactions between the nitrogen-containing groups and POM clusters. These interactions contribute to the structural stability and uniform dispersion of the POMs within the fluoropolymer network. The XRD patterns (Fig. 3d) show that FPPC exhibits a broad amorphous halo, which is typical of polymeric materials. After loading the POMs, sever-

https://doi.org/10.1007/s10118-026-3790-7

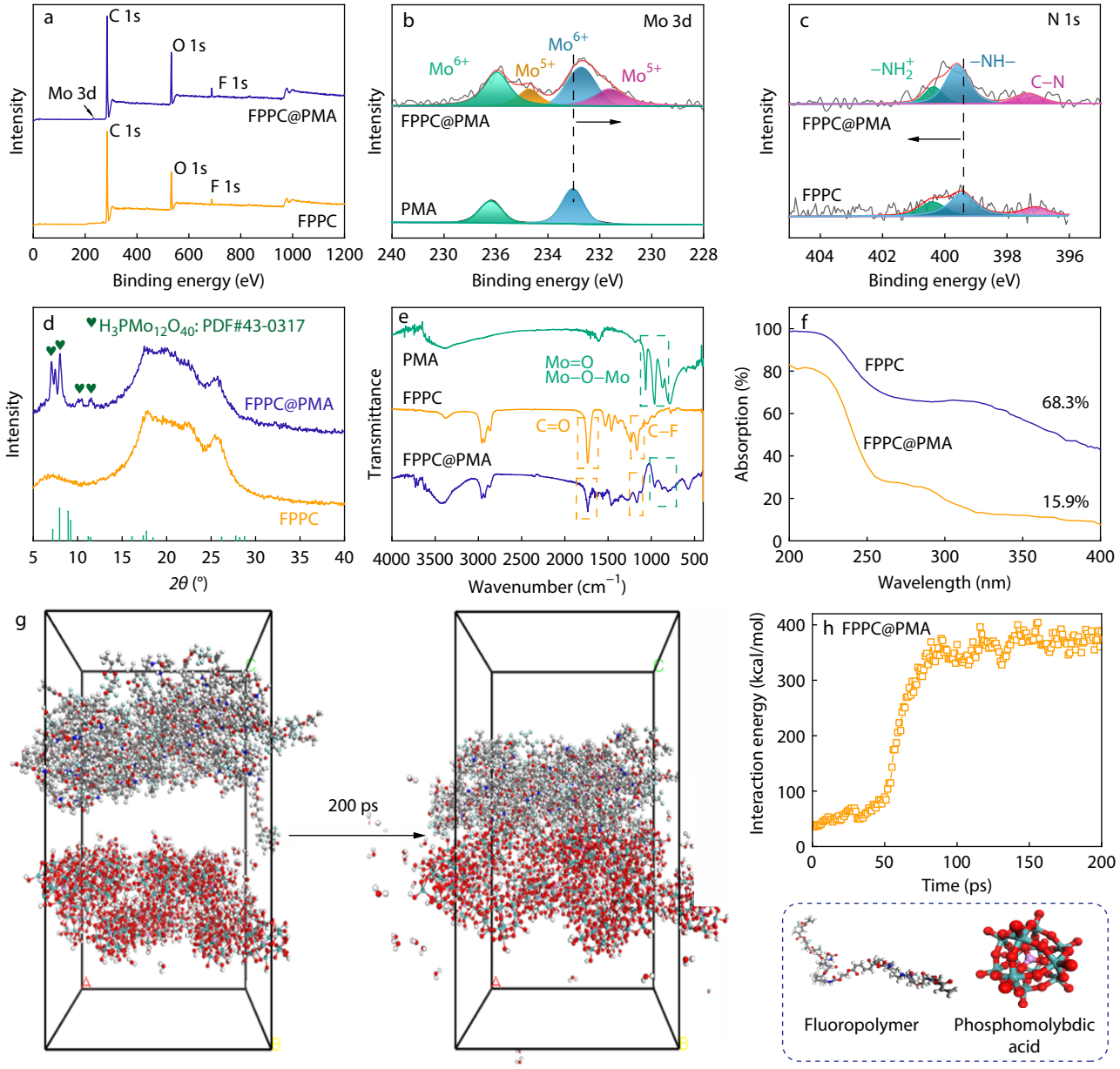

Fig. 3 Structural, optical, and interfacial characterization of FPPC@PMA and FPPC. (a) XPS survey spectra; (b) Mo 3d XPS spectra; (c) N 1s XPS spectra; (d) XRD patterns; (e) FTIR spectra; (f) UV-Vis absorption spectra; (g) Molecular dynamics simulation snapshots; (h) Time-dependent interaction energy.

al weak diffraction features consistent with phosphomolybdic acid references appeared, confirming the presence of crystalline POM domains while maintaining the overall amorphous polymer framework. This indicates that the POM structure was preserved during the HIPE polymerization.

The FTIR spectra (Fig. 3e) further confirm the chemical structure of the coatings. The bands at around 1200 cm^{-1} correspond to the C—F stretching vibrations of the fluoropolymer backbone, while the characteristic Mo—O and Mo—O—Mo vibrations appear after POM incorporation.[13,14] Notably, slight shifts in these peaks suggest strong interfacial interactions between the fluoropolymer matrix and POM clusters, which may enhance the coating stability and functionality UV-Vis absorption spectra (Fig. 3f) revealed that FPPC@PMA exhibited significantly enhanced light absorption compared to FPPC. The absorption intensity increased from 15.9% to 68.3% in the UV region, demonstrating the strong photoresponse of the POM species. This enhanced light-harvesting capability provides an optical basis for the photochromic behavior of the coating. Molecular dynamics simulations were performed to understand the interfacial interactions between the fluoropolymer chains and phosphomolybdic acid clusters (Fig. 3g). Over a simulation time of 200 ps, the POM molecules gradually approached and anchored onto the polymer surface, indicating spontaneous adsorption driven by intermolecular interactions. Fig. 3(h) shows a rapid increase, followed by stabilization, suggesting the formation of a thermodynamically favorable binding state. The strong

https://doi.org/10.1007/s10118-026-3790-7

interaction energy indicates robust interfacial coupling between the fluoropolymer and POM clusters, which explains the stability and uniform dispersion of the POMs within the coating.[15]

Surface Wetting Property of FPPC@PMA

The wettability of the coating was first evaluated using static and dynamic water contact angle measurements.[16–18] As shown in Fig. 4(a), a water droplet maintains a nearly spherical shape on the coating surface with a contact angle of 152°, indicating the typical superhydrophobic nature of the material. In addition to the high water contact angle, the FPPC@PMA coating exhibited a low sliding angle of 7.41°, indicating minimal interaction between the water droplets and surface. A compression–release test was conducted to further examine the wetting stability (Fig. 4b). When the droplet was pressed with the probe, it retained its spherical shape without spreading. After removing the probe, the droplet rapidly recovered and detached from the surface, suggesting an extremely low adhesion.[19]

The dynamic behavior of the droplets was further investigated using a high-speed camera (Fig. 4c). Upon impact, the droplet rapidly rebounded from the surface with minimal spreading or pinning, demonstrating excellent water repellency and low energy dissipation, which are characteristic features of superhydrophobic surfaces.

To evaluate the chemical durability of FPPC@PMA, the

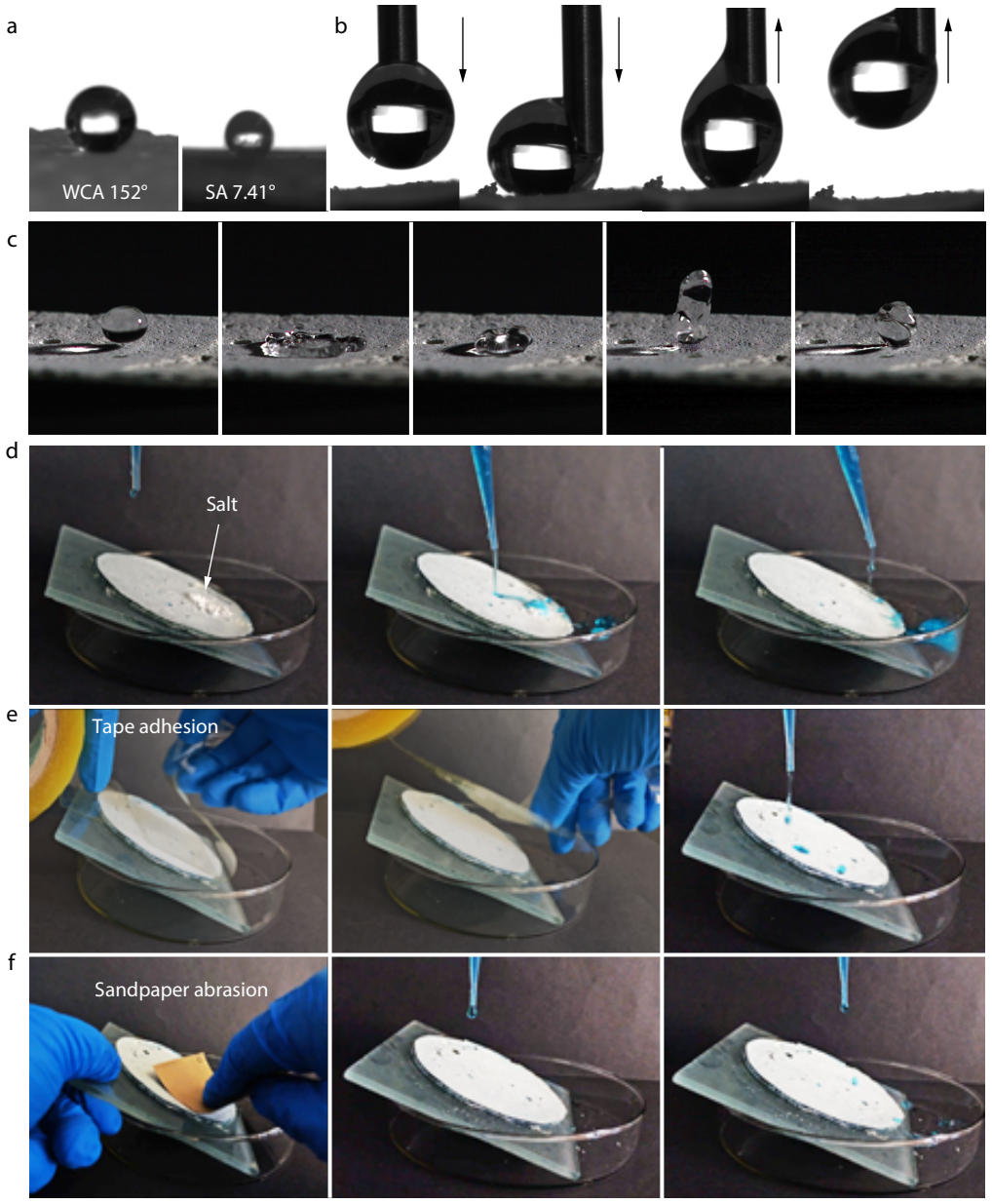

Fig. 4 Superhydrophobic performance and durability tests of the coating. (a) Static water contact angle and sliding angle test; (b) Water droplet compression-release process; (c) High speed camera images capturing the droplet impact and rebound; (d) Wetting behavior test after salt contamination; (e) Wetting performance test after tape peeling; (f) Wetting performance test after sandpaper abrasion.

coating was immersed in acidic and alkaline solutions of varying pH values. As shown in Fig. S6 (in ESI), the water contact angle of the coating remained consistently above 150°. The excellent chemical stability is attributed to the robust fluoropolymer backbone and the integrated porous structure formed *via* the HIPE template strategy, which effectively maintains the hierarchical roughness and low surface energy under corrosive conditions.

The practical durability, contamination resistance, adhesion stability, and mechanical robustness were examined through salt deposition, tape peeling, and sandpaper abrasion tests (Figs. 4d–4f). Even after the salt particles were deposited on the surface, the droplets remained spherical and easily rolled off (Fig. 4d), indicating a strong anti-fouling capability. After repeated tape adhesion–peeling cycles, the coating still exhibited a high contact angle (Fig. 4e), which confirms the strong interfacial adhesion between the coating and the substrate. Moreover, the coating maintained its hydrophobicity after sandpaper abrasion (Fig. 4f), demonstrating its excellent mechanical durability.[20] As shown in Figs. S3 and S4 (in ESI), the FPPC@PMA coating maintains excellent superhydrophobicity throughout the abrasion process. Interestingly, a slight increase in the WCA was observed during the initial abrasion cycles. This phenomenon was attributed to the monolithic porous architecture generated by the HIPE templating strategy. Abrasion exposes fresh fluoropolymer skeletons and additional micro/nano hierarchical structures from the interior, thereby enhancing air trapping and stabilizing the Cassie–Baxter wetting state. Consequently, hydrophobicity remained stable or slightly improved after moderate abrasion. SEM observations were performed after the durability tests to further evaluate the structural stability of the coating. As shown in Fig. S5 (in ESI), the lotus leaf-inspired hierarchical micro/nanostructures are largely retained after the salt deposition, tape-peeling, and abrasion treatments.

Overall, the HIPE-derived fluoropolymer-supported POM coating not only exhibited typical superhydrophobic characteristics, but also possessed strong anti-contamination ability, adhesion stability, and mechanical robustness, highlighting its potential for practical applications in harsh environments.[20] These robust properties are essential for ensuring the long-term reliability and functional integrity of advanced coatings, particularly when subjected to the synergistic stresses of physical abrasion and chemical contamination in real-world scenarios.

Photochromic Properties and Applications of FPPC@PMA

As shown in Fig. 5(a), the FPPC@PMA system was constructed from a fluorinated polymer network and polyoxometalate clusters (centered on Mo) *via* hydrogen bonding and coordination interactions.[7,21] This architecture not only provides a confined and stable microenvironment, but also facilitates the efficient transfer of photoinduced electrons between the organic chains and inorganic clusters. Upon ultraviolet (UV) irradiation, the Mo(VI) species are preferentially reduced at coordinatively unsaturated sites to generate Mo(V), accompanied by local electron density redistribution and subtle conformational adjustments. These changes lead to enhanced absorption in the visible region and a pronounced color variation. In the presence of oxygen, Mo(V) was reoxidized to Mo(VI), enabling full recovery of the system. This reversible "photo-reduction–oxidation regeneration" cycle endows the material with dynamically tunable optical properties. CIE (International Commission on Illumination) chromaticity analysis (Fig. 5b) quantitatively corroborated these observations. A significant shift in color coordinates was observed before and after irradiation, with the overall color evolving from a high-luminance region toward lower brightness and longer wavelengths. This indicates enhanced visible-light absorption and increased color purity. Such pronounced chromatic transition reflects the tunability of electronic transitions within the system and provides a reliable basis for visual information encoding.

Time-dependent photoresponse experiments (Fig. 5c) further elucidate the kinetics of the process. Under UV irradiation at 365 nm (80 mW·cm^{-2}), the material exhibited gradual deepening of color as the exposure time increased from 0 s to 180 s, indicating a cumulative photoreduction process. Upon subsequent exposure to oxygen, the color progressively recovers, demonstrating that the oxidation process is time dependent and controllable. This reversible "writing (UV)–erasing (O_2)" behavior exhibits excellent cycling stability and reproducibility, confirming that the material maintains structural integrity without significant irreversible degradation during repeated redox cycles.

A mask-assisted patterning strategy was demonstrated by leveraging this reversible photoresponsive property (Fig. 5d). By combining UV irradiation with a hollow mask, high-resolution patterns, such as QR codes, can be precisely generated on the material surface and subsequently read *via* scanning. These patterns can be erased by oxygen treatment, enabling rewritable information storage. Compared with conventional printing or chemical etching techniques, this non-contact and reprogrammable approach offers several advantages, including operational simplicity, reversibility, and enhanced safety.

In practical applications (Fig. 5e), the FPPC@PMA material was integrated into a flexible substrate for wearable use. The material exhibited distinct color changes under natural sunlight and could spontaneously recover in ambient air, demonstrating real-time responsiveness to UV exposure. These results highlight the potential for UV detection, smart protection, and wearable sensing devices.

Fig. 6(a) illustrates the cycling stability of the FPPC@PMA system during repeated "UV writing–O_2 erasing" processes. The color counting values exhibit highly reversible periodic switching between the high (about 100%) and low (about 0%) states over 20 cycles, with negligible attenuation or baseline drift. Both the peak and valley values remained essentially constant throughout the cycling test, indicating the excellent fatigue resistance and reversibility of the Mo(VI)/Mo(V) redox process. The corresponding optical images further confirm the rapid and consistent transition between the dark and light states. Notably, no obvious response delay or degradation was observed, suggesting that the material maintained its structural integrity without significant irreversible side reactions during repeated photoinduced redox cycles. RGB image analysis was employed to quantitatively characterize the photochromic response. The RGB values extracted from the photographs acquired under identical conditions were used to calculate RGB-based color intensity. The variation in this parameter during UV irradiation and subsequent recovery re-

https://doi.org/10.1007/s10118-026-3790-7

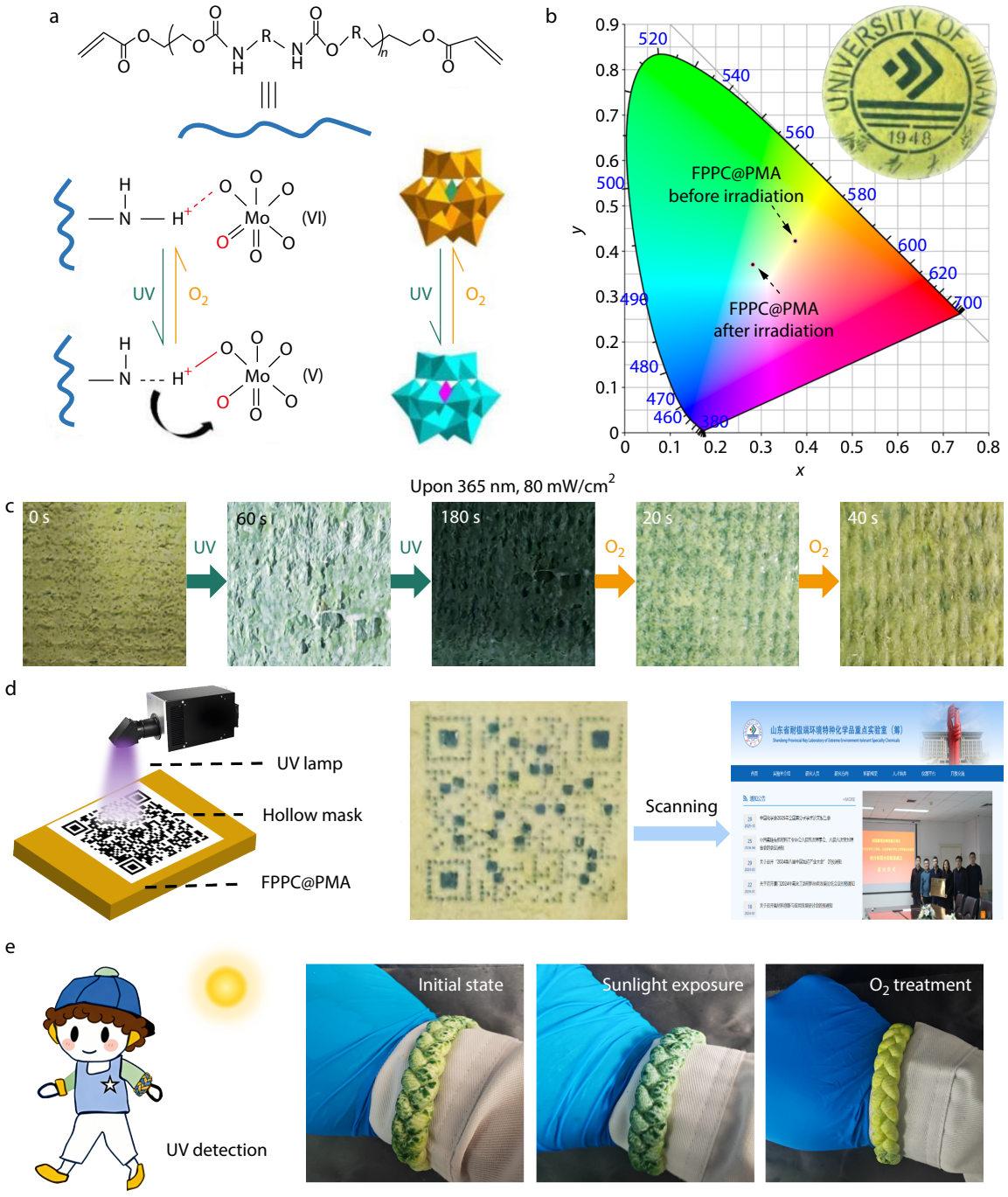

Fig. 5 Photochromic mechanism and applications of FPPC@PMA coating. (a) Schematic of photochromic mechanism; (b) CIE chromaticity diagram and sample photographs before and after UV irradiation; (c) Time-dependent photochromic and recovery process under UV irradiation; (d) Demonstration of image storage application; (e) UV detection application under sunlight..

flects the reversible photochromic behavior of the FPPC@PMA coating. Fig. 6(b) compares the color counting performance of FPPC@PMA with that of previously reported photochromic materials. The FPPC@PMA system achieved a high color counting value of approximately 97%, outperforming typical photochromic wool fabric (72%), cotton fabric (72%), coated cotton fabric (83%), and photochromic paper (76%), and surpassing most nanofiber membrane systems (about 90%).[22–26] This superior performance indicates enhanced color contrast, improved recognition accuracy, and a higher signal-to-noise ratio. This performance enhancement can be attributed to several factors: (i) the organic–inorganic hybrid structure facilitates efficient electron transfer, leading to a stronger photoresponse; (ii) the fluorinated polymer network provides a hydrophobic and confined microenvironment that suppresses side reactions and improves reversibility; (iii) the uniform distribution of Mo-based active sites ensures consistent and reproducible optical responses.

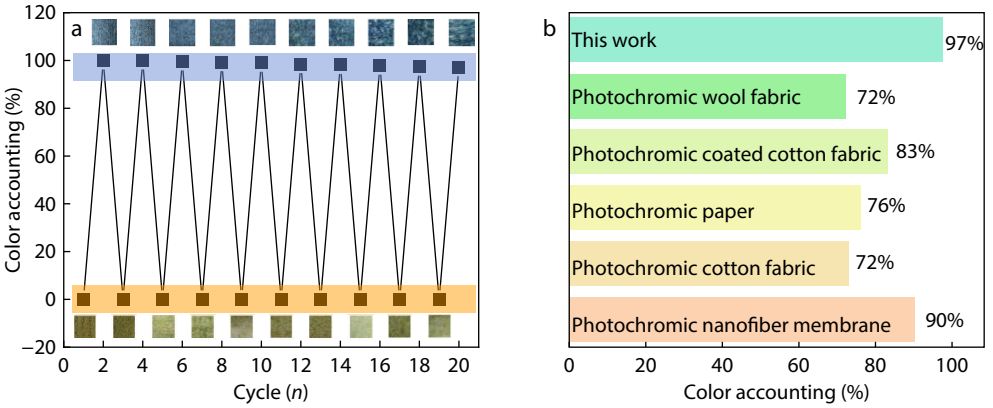

Fig. 6 Cycling stability and color counting performance of FPPC@PMA. (a) Reversible color switching under repeated UV writing–O_2 erasing cycles with corresponding optical images; (b) Comparison of color counting performance with previously reported photochromic materials.

To further evaluate the performance of the FPPC@PMA coating, a systematic comparison with representative POM-based photochromic materials and superhydrophobic photochromic coatings reported in the recent literature was conducted (Table S1 in ESI).

Although a variety of photochromic systems have been developed, most studies have focused primarily on enhancing the photochromic response without simultaneously considering the surface wettability and mechanical durability. In contrast, the FPPC@PMA coating combines reversible photochromic functionality with superhydrophobicity and robust mechanical stability through an HIPE-derived interconnected porous architecture.

More importantly, the HIPE strategy enables the incorporation of hydrophilic POMs while preserving the hierarchical micro/nanostructure required for superhydrophobicity, which remains a significant challenge in multifunctional surface design.

Overall, the FPPC@PMA material demonstrated outstanding cycling durability and superior color discrimination capability compared to existing systems, highlighting its strong potential for applications in reliable information storage, rewritable optical devices, and photoresponsive sensing technologies.

CONCLUSIONS

In this study, a fluoropolymer-supported polyoxometalate composite coating (FPPC@PMA) was successfully fabricated using a high internal phase emulsion (HIPE) templating strategy. In this system, an oil phase consisting of poly(urethane diacrylate) (PUDA) and the fluorinated monomer HFBA encapsulates an aqueous phosphomolybdic acid (PMA) solution to form a stable water-in-oil (W/O) emulsion. After polymerization, a biomimetic hierarchical porous structure with three-dimensional interconnected pores was formed. The PMA clusters were uniformly immobilized within the fluorinated polymer matrix, enabling the coating to maintain micro/nano hierarchical roughness while introducing reversible photochromic functionality. Owing to the hierarchical porous structure derived from the HIPE template and intrinsically low surface energy of the fluoropolymer, the obtained coating exhibited excellent superhydrophobicity with a static water contact angle of 152°. Moreover, the coating demonstrated good mechanical durability during sandpaper abrasion and tape-peeling tests, indicating its robust structural stability. In addition, redox-active PMA endowed the coating with a sensitive and reversible photochromic response under ultraviolet (UV) irradiation, enabling potential applications in UV detection and information encryption. Molecular dynamics (MD) simulations further revealed the interfacial interactions between the polymer chains and PMA clusters, providing theoretical insights into the structural stability and uniform dispersion of the composite system. Overall, this study presents a synergistic strategy that combines HIPE structural engineering with functional component integration, offering a promising approach for the development of durable multifunctional surfaces with superhydrophobic and photoresponsive properties for applications in intelligent protection and harsh environments.

Conflict of Interests

The authors declare no interest conflict.

Electronic Supplementary Information

Electronic supplementary information (ESI) is available free of charge in the online version of this article at http://doi.org/10.1007/s10118-026-3790-7.

Data Availability Statement

The data that support the findings of this study are available from the corresponding author upon reasonable request.

ACKNOWLEDGMENTS

This work was financially supported by the Natural Science Foundation of Shandong Province (No. ZR2023LFG004), the National Natural Science Foundation of China (No. 52173168), Taishan Scholars Program project (No. TSQN tstp20221131), Science and Technology Program of the University of Jinan (No. XKY22210), and University of Jinan Disciplinary Cross Convergence Construction Project 2023 (No. XKJC-202302).

Graphical Abstract

Constructing Superhydrophobic High-internal-phase Emulsion Fluoro-coatings from Hydrophilic Polyoxometalates for Durable Photochromic Functionality

Pei-Ze Yang, Xiao-Shuang Li, Bo-Yu Lei, Yi-Lin Tang, Bing Geng, Guang-Hui Cui, and Mei Yan

University of Jinan; China National Petroleum Corporation

A high-internal-phase emulsion-templated fluoropolymer framework enables the stable immobilization of hydrophilic phosphomolybdic acid while preserving hierarchical roughness, yielding a monolithic coating with durable superhydrophobicity and reversible photochromic performance for UV sensing and information encryption.

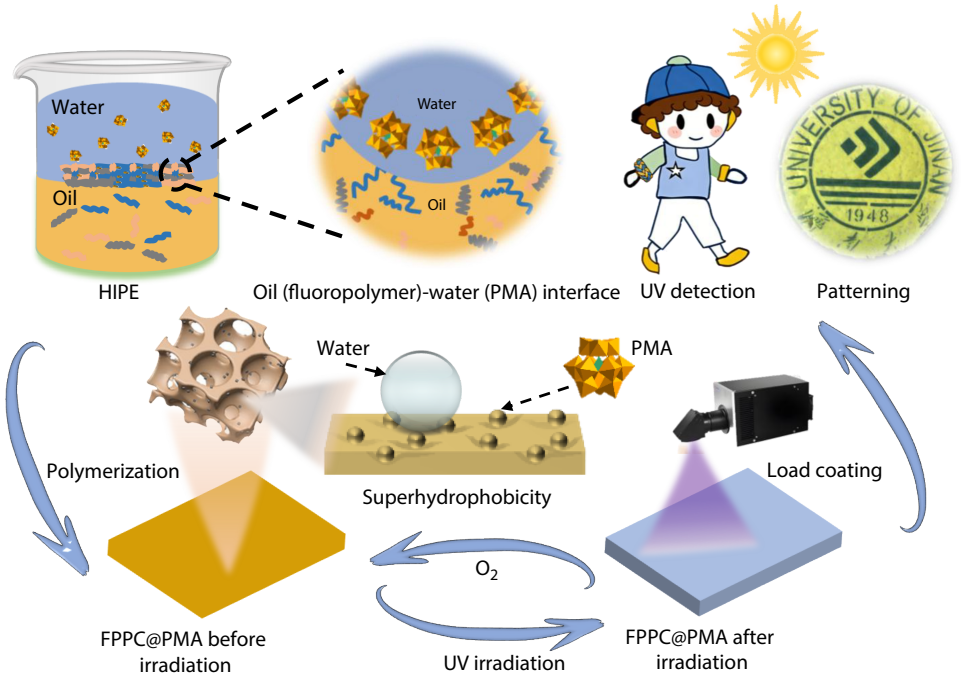

Chinese J. Polym. Sci., 2026 *https://doi.org/10.1007/s10118-026-3790-7*

REFERENCES

1 Wang, D.; Huang, J.; Guo, Z. Tomato-lotus inspired edible superhydrophobic artificial lotus leaf. *Chem. Eng. J.* **2020**, *400*, 125883.
2 Zheng, X.; Tang, Y.; Bai, Y. UV-curable optical transparent, aging resistance, liquid-repellent coatings based on a novel photosensitive fluorinated polysiloxane with long perfluoroalkyl side chains. *Eur. Polym. J.* **2022**, *175*, 111324.
3 Wan, J.; Xu, J.; Zhu, S.; Li, J.; Ying, G.; Wang, B.; Chen, K. Easily prepared superhydrophobic photochromic composite and its application in waterproof rewritable paper. *Chem. Eng. J.* **2022**, *444*, 136604.
4 Li, L.; Yu, Y. T.; Zhang, N. N.; Li, S. H.; Zeng, J. G.; Hua, Y.; Zhang, H. Polyoxometalate (POM)-based crystalline hybrid photochromic materials. *Coord. Chem. Rev.* **2024**, *500*, 215526.
5 Sun, Y.; Yang, M.; Liu, T.; Ying, J.; Tian, A.; Wang, X. Four multi-stimuli-responsive color-changing materials based on Anderson-viologens for erasable inkless printing, UV detectors and gradient detection of amine gases. *Spectrochim. Acta Part A Mol. Biomol. Spectrosc.* **2025**, *332*, 125826.
6 Wei, Y.; Han, B.; Dong, Z.; Feng, W. Phosphomolybdic acid-modified highly organized TiO_2 nanotube arrays with rapid photochromic performance. *J. Mater. Sci. Technol.* **2019**, *35*, 1951–1958.
7 Ganapathy, S.; Fournier, M.; Paul, J. F.; Delevoye, L.; Guelton, M.; Amoureux, J. P. Location of protons in anhydrous keggin heteropolyacids $H_3PMo_{12}O_{40}$ and $H_3PW_{12}O_{40}$ by $^1H\{^{31}P\}/^{31}P\{^1H\}$REDOR NMR and DFT quantum chemical calculations. *J. Am. Chem. Soc.* **2002**, *124*, 7821–7828.
8 Yang, P.; Li, X.; Zhang, Z.; Zhu, M.; Lei, B.; Geng, B.; Cui, G.; Yan, M. Phosphomolybdic acid induced water clusters formation in freezing seawater: enabling ultra-low enthalpy and efficient solar evaporation. *Adv. Funct. Mater.* **2026**, *36*, e14707.
9 Tan, Y.; Wang, F.; Sun, R. Y.; Wang, M.; Song, F.; Wang, Y. Z. Crystalline alkyl side chain enhanced hydrophobicity–oleophobicity for transparent and durable low-surface-energy coatings based on short fluorinated copolymers. *Macromolecules*

2024, *57*, 5189–5199.
10 Wu, M.; Li, X.; Wen, D.; Ma, Y.; Yang, P.; Zhang, Z.; Geng, B.; Li, H. Fabrication of fluorinated superhydrophobic oil-absorption cabins with controllable movement, elasticity, and wear resistance. *J. Water Process Eng.* **2024**, *66*, 106081.
11 Liao, J. Z.; Liu, S. J.; Ke, H. Excited-state proton transfer in a photoacid-based crystalline coordination compound: reversible photochromism, near-infrared photothermal conversion, and conductivity. *Inorg. Chem.* **2023**, *62*, 16825–16831.
12 Turek, W.; Lapkowski, M.; Stolarczyk, A.; Debiec, J. EPR and XPS measurements of polymeric catalysts doped with hereopolyacids in oxygen adsorption studies. *Appl. Surf. Sci.* **2005**, *252*, 801–806.
13 Cheng, S.; Liu, C.; Li, Y.; Tan, H.; Wang, Y.; Li, Y. Polyoxometalates-modulated hydrophilic-hydrophobic composite interfacial material for efficient solar water evaporation and salt harvesting in high-salinity brine. *Energy Environ. Mater.* **2024**, *7*, e12647.
14 Meng, R.; Lyu, J.; Lu, Y.; Salimi, M.; Zhu, B.; Macharia, D. K.; Zhang, L.; Amidpour, M.; Zou, L.; Chen, Z. Growth of phosphomolybdate-carbon hybrid nanorod array on carbon-fiber cloth with enhanced light-trapping and decreased water-evaporation enthalpy for constructing efficient salt-free hanging evaporator. *Chem. Eng. J.* **2023**, *476*, 146756.
15 Sun, W.; Li, H.; Li, H.; Li, S.; Cao, X. Adsorption mechanisms of ibuprofen and naproxen to UiO-66 and UiO-66-NH2: batch experiment and DFT calculation. *Chem. Eng. J.* **2019**, *360*, 645–653.
16 Hou, S.; Noh, I.; Shi, X.; Wang, Y.; Do Kim, H.; Ohkita, H.; Wang, B. Facile fabrication of flexible superhydrophobic surfaces with high durability and good mechanical strength through embedding silica nanoparticle into polymer substrate by spraying method. *Colloids Surf. A Physicochem. Eng. Aspects* **2023**, *664*, 131181.
17 Zhou, N.; Hou, S.; Noh, I.; Liu, Q.; Wang, Y.; Do Kim, H.; Zhou, Q.; Ohkita, H.; Wang, B. Constructing robust and multifunctional superamphiphobic surfaces by using two different nanostructures of silicon dioxide. *Langmuir* **2025**, *41*, 6376–6388.
18 Chang, C.; Noh, I.; Zhou, N.; Jeon, J.; Wang, Y.; Do Kim, H.; Liu, Q.; Ohkita, H.; Tao, X.; Wang, B. Construction of robust superhydrophobic surfaces with electrothermal, photothermal properties using simple spraying method. *Surf. Interfaces* **2024**, *52*, 104879.
19 Fan, H. Q.; Lu, P.; Zhu, X.; Behnamian, Y.; Li, Q. Development of superhydrophobic and corrosion resistant coatings on carbon steel by hydrothermal treatment and fluoroalkyl silane self-assembly. *Mater. Chem. Phys.* **2022**, *290*, 126569.
20 Wang, P.; Zhang, X.; Wang, Z.; Chen, T.; Zhang, H.; Duan, W.; Han, H. A robust superhydrophobic smart coating with reversible thermochromic and photochromic property. *J. Bionic Eng.* **2022**, *19*, 1589–1600.
21 Zhang, Q.; Wang, R.; Lu, Y.; Wu, Y.; Yuan, J.; Liu, J. Highly efficient photochromic tungsten Oxide@PNIPAM composite spheres with a fast response. *ACS Appl. Mater. Interfaces* **2021**, *13*, 4220–4229.
22 You, M.-H.; Li, M.-H.; Di, Y.-M.; Wang, Y.-W.; Lin, M.-J. Switching on room-temperature phosphorescence of photochromic hybrid heterostructures by anion-π interactions. *Dyes Pigm.* **2020**, *173*, 107943.
23 Bao, B.; Bai, S.; Fan, J.; Su, J.; Wang, W.; Yu, D. A novel and durable photochromic cotton-based fabric prepared *via* thiol-ene click chemistry. *Dyes Pigm.* **2019**, *171*, 107778.
24 Sun, M.; Lv, J.; Xu, H.; Zhang, L.; Zhong, Y.; Chen, Z.; Sui, X.; Wang, B.; Feng, X.; Mao, Z. Smart cotton fabric screen-printed with viologen polymer: photochromic, thermochromic and ammonia sensing. *Cellulose* **2020**, *27*, 2939–2952.
25 Sartzi, H.; Miras, H. N.; Vilà-Nadal, L.; Long, D.-L.; Cronin, L. Trapping the δ isomer of the polyoxometalate-based Keggin cluster with a tripodal ligand. *Angew. Chem. Int. Ed.* **2015**, *54*, 15488–15492.
26 Li, D.; Wei, J.; Dong, S.; Li, H.; Xia, Y.; Jiao, X.; Wang, T.; Chen, D. Novel PVP/HTA hybrids for multifunctional rewritable paper. *ACS Appl. Mater. Interfaces* **2018**, *10*, 1701–1706.

https://doi.org/10.1007/s10118-026-3790-7